Effect of chopped ZrO_2 fiber content on the microstructure and properties of CaO-based integral ceramic mold

Qiang Yang
Xi'an Jiaotong University
Fu Wang (fuwang@xjtu.edu.cn)
Xi'an Jiaotong University
Dichen Li
Xi'an Jiaotong University

Research Article

Keywords: ZrO2 fiber, calcium oxide, gel-casting, microstructure, properties

Posted Date: September 21st, 2020

DOI: https://doi.org/10.21203/rs.3.rs-80172/v1

Abstract

A chopped ZrO_2 fiber ($ZrO_{2\ (f)}$) reinforced CaO-based integral ceramic mold was successfully fabricated by stereolithography (SLA) and tert-butyl alcohol (TBA)-based gel-casting, and the effect of chopped $ZrO_{2\ (f)}$ content on properties of the ceramic mold was investigated. The results show that the $ZrO_{2\ (f)}$ content had a significant effect on the viscosity of CaO-based ceramic slurry, which directly affects the filling ability of the ceramic slurry in complex structures of the integral mold. The tiny structures of the ceramic mold cannot be filled completely with a $ZrO_{2\ (f)}$ content exceed 3 vol%. When the content of $ZrO_{2\ (f)}$ was 3 vol%, the ceramic slurry could meet the requirement of gel-casting with a viscosity of 0.84 Pa·s. The $ZrO_{2\ (f)}$ content played an important role in tailoring properties of the ceramic mold, the sample fabricated with 3 vol% fiber content showed a harmonious microstructure and exhibited an excellent comprehensive performance with a room temperature (25 ºC) bending strength of 22.88 MPa, the elevated temperature bending strength (1200 ºC) of 15.74 MPa, the elevated temperature (1200 ºC) deflection of 0.86 mm and the sintering shrinkage of 0.40%, which can meet the requirements of casting very well.

1. Introduction

CaO has long been considered as an attractive refractory for application in metallurgical and ceramics industries because of the global abundant sources of high-purity limestone, as well as its advantages of high melting temperature, low vapor pressure, and excellent thermodynamic stability [1–5]. In recent years, CaO was studied as a potential ceramic core material for investment casting due to the reaction-resistance to molten active alloy [6–8], easy dissolution compared to common ceramic core materials, such as fused silica or alumina [9–11], and approximating the thermal expansion coefficient of superalloys [12]. However, in spite of these primary advantageous properties, the application of CaO is inhibited due to its hydration susceptibility in atmospheric moisture [2–5, 13–14], which increased the difficultly of fabricating CaO ceramics as well. Most existing methods for forming CaO ceramic, such as hot-pressing [1], cold-pressing [3–5], can only fabricate simple architectures, which makes them untenable for generating complex ceramic structures.

The rapid integral fabrication technique (RIFT) based on stereolithography (SLA) and non-aqueous gel-casting technology, provides a new approach for fabricating complex ceramic components, especially the ceramic molds of hollow turbine blades [15–18]. The tert-butyl alcohol (TBA) is selected as solvent, on the one hand because it can effectively avoid the hydrolysis of CaO powder, and on the other hand because of its high saturation vapor pressure and low surface tension force, the green body can be easily dried with a small shrinkage and deformation [19]. In order to meet the requirement of investment casting, the ceramic mold must has a good performance in mechanical properties and no structure defects, such as cracks, severe deflection or shrinkage deformation. However, cracking often occurs during the pre-sintering of RIFT process. In this stage, integrity of ceramic mold can be only maintained by the particle packing effects because the gel networks were burnt off. Therefore, the slender structures may be broken by gravity and the thin-wall structures also may be broken by the stress caused by pyrolysis of resin

prototype. Moreover, the integral ceramic mold always has a slightly poor mechanical properties, a lager deflection and sintering shrinkage. The unacceptable drawbacks for investment casting of ceramic mold can be overcome by incorporating particulate, whisker or fiber into the base materials to form ceramic matrix composites [20, 21]. Especially using chopped fibers, the ceramic can not only be strengthened in isotropic properties due to the homogenous distribution, but also the ceramic mold with complex structures can be formed by conventional manufacturing techniques, such as slip casting or gel-casting [22, 23].

In this work, the chopped $ZrO_{2\ (f)}$ was selected to reinforce the CaO-based integral ceramic mold due to its high melting point, excellent strength and toughness, low thermal conductivity, super corrosion and oxidation resistance [24]. In addition, the chopped $ZrO_{2\ (f)}$ can be well retained during the sintering of the CaO matrix, because it does not react with the CaO matrix at the lower sintering temperature unlike the silica or alumina fibers. The CaO-based integral ceramic molds are fabricated by RIFT technique with the TBA-based gel-casting. The effects of chopped $ZrO_{2\ (f)}$ content on the viscosities and filling ability of the slurries, the microstructures, mechanical properties, deflection and sintering shrinkage of ceramic mold were investigated, and the reinforcing mechanism of chopped $ZrO_{2\ (f)}$ reinforced porous CaO ceramic mold was also discussed.

2. Material And Methods

2.1 Raw materials

A commercial CaO powders (mean particle diameter = 22.05 μm, purity ≥ 99%, Xing Tai special ceramics Co. Ltd., Xi'an, China), a commercial fused MgO powders (mean particle diameter = 23.92 μm, purity ≥ 99%, Henghai magnesium industry co. Ltd., Lianyungang, China) and the chopped ZrO_2 fiber (mean diameter and length are 5–8 μm and 200 μm, respectively, purity ≥ 99%, Shandong Huolong Ceramic Fiber Co., Ltd., Jinan, China) were used as the raw materials. Zirconium powder (AR, Western BaoDe Technologies Co., Ltd., Xi'an, China) with a mean particle diameter of 1 μm was used as the sintering additive. The morphology of the CaO powders, MgO powders and $ZrO_{2\ (f)}$, the particle size distribution of the CaO powders, MgO powders and the aspect ratio of $ZrO_{2\ (f)}$ were shown in Fig. 1.

2.2 Experimental procedure

The premixed solution was prepared by dissolving N, N-dimethylacrylamide (DMAA) and N, N-methylene diacrylamide (MBAM) into the Tert-butyl alcohol (TBA) with the weight ratio of DMAA: MBAM: TBA = 24:2:100. 3 wt. % polyvinyl pyrrolidone (PVP K30) with respect to the total mass of powders was add into the premixed solution as dispersant. All the chemical reagents are of AR purity and provided by Sinopharm Chemical Reagent Ltd, Shanghai, China. Due to the serious agglomeration of the chopped zirconia fibers, the $ZrO_{2\ (f)}$ must be pre-dispersed before use. An appropriate amount of $ZrO_{2\ (f)}$ need to be added into absolute ethyl alcohol, subsequently placed in an ultrasonic disperser for 2–4 hours, and dried finally. Then the appropriate amount CaO, MgO and Zr powders and a certain amount of processed ZrO_2

$_{(f)}$ were added into the premixed solution by mechanical stirring, followed by the ball milling for 40 minutes. The prepared slurries exhibited a good flow-ability and stability were degased for more than 5 min. After adding an appropriate amount of initiator and catalyst solutions, the mixed slurry was poured into the SLA resin mold fabricated by SPS600B Rapid Prototyping Machine (Shaanxi Hengtong Intelligent Machine Co., Ltd, Xi'an, China) using photosensitive resin (SPR 8981; Zheng bang Ltd., Zhuhai, China) under vacuum and vibration conditions. After the polymerization of the monomers, the green body was put into the vacuum drying oven (Taisite Instrument Co., Ltd., Tianjin, China) at 40 °C for 48 hours. At last, an integral CaO-based ceramic mold was obtained after sintered at 1400 °C and kept for 3 hours. Figure 2 shows the fabrication flow chart of the CaO-based integral ceramic mold. During the fabrication process, the total solid loading (the solid loading of CaO particles, MgO particles and $ZrO_{2\ (f)}$) of the slurry was fixed at 56 vol%, while the $ZrO_{2\ (f)}$ varied from 0 vol% to 4 vol%. The component of the composite powders was shown in Table 1.

Table 1
Component of the composite powders

Sample No.	Volume fraction (vol%)			
	CaO (22.05 μm)	MgO (23.92 μm)	Zr (5 μm)	$ZrO_{2(f)}$
A	42.00	12.00	2.00	0.00
B	41.00	12.00	2.00	1.00
C	40.00	12.00	2.00	2.00
D	39.00	12.00	2.00	3.00
E	38.00	12.00	2.00	4.00

2.3 Characterization and testing

The particle sizes of the powders were measured by the Laser Particle Sizer (BT-9300S, Better Instruments Co., Ltd., Dandong, China). The viscosity of ceramic slurries was tested by the Digital rotational viscometer (SNB-3, Shanghai NiRun Intelligent Technology Co., Ltd., Shanghai, China). The structures of the fine structure samples and the integral ceramic mold were investigated by the micro X-ray imaging system (Y. Cheetah, YXLON, Hamburg, Germany) with a scanning resolution of 50 μm. The phase composition was identified by X-ray diffraction (XRD) (X'Pert Protype, PANalytical BV, Almelo, Netherlands). The microstructure and elemental composition of samples were investigated by the field emission scanning electron microscope (SEM) (SU-8010, Hitachi Ltd., Tokyo, Japan). The bending strengths of samples were tested by a three-point bending test machine (HSST-6003QP, Sinosteel Luoyang Institute of Refractories, Luoyang, China) with a span distance of 30 mm at a crosshead speed

of 6 mm/min using samples of a nominal size of 4 mm × 10 mm × 60 mm. The apparent porosity of sintered bodies were measured by immersion method in absolute ethyl alcohol under vacuum using Archimedes' principle. The sintering shrinkage of samples was calculated according to the following Eq. (1).

$$\varepsilon = {L_1 - L_2}/{L_1} \times 100\% \quad (1)$$

Where ε is the shrinkage of sample, L_1 is the length of sample before sintering, L_2 is the length of sample after sintering.

3. Results And Discussion

3.1 Effect on viscosity and filling ability of the slurry

At present, a large number of complex parts, such as aero engine blades, impellers, etc., are produced by investment casting technology. Therefore, the structure of ceramic molds have also become very complex, containing many tiny structures, as shown in the Fig. 3 (a). It is always very difficult to fill the tiny and complex structures in the ceramic mold sufficiently during the fabrication process of the integral ceramic mold by RIFT process. Some insufficient filled situations often occur in these tiny structures, which leads to the loss of the structural integrity of the mold and the failure of ceramic mold fabrication. The structural integrity of the ceramic mold is directly determined by the filling ability of the ceramic slurry, depending on the viscosity of the ceramic slurry. Generally speaking, in order to obtain a complete filling of the fine structure, the viscosity of the ceramic slurry is must less than 1 Pa·s in the gel-casting process [25]. Since the viscosity of ceramic slurry is very sensitive to the content of $ZrO_{2\ (f)}$, it is very important to obtain an appropriate $ZrO_{2\ (f)}$ addition amount to realize the tiny structures duplication without defects.

Figure 3b-g shows the effect of $ZrO_{2\ (f)}$ content on viscosity and filling ability of the slurries. As can be seen from Fig. 3b, the viscosity of slurries increased gradually with the increasing of $ZrO_{2\ (f)}$ content. When the $ZrO_{2\ (f)}$ content reaches 4 vol%, the viscosity exceed 1Pa·s, the limit of slurry viscosity in gel-casting process [25]. As shown in Fig. 3c - Fig. 3g, the tiny structures could be filled perfectly, when the $ZrO_{2\ (f)}$ content was not exceeding 3 vol%. However, some insufficient filled areas were found in the tiny structures as the $ZrO_{2\ (f)}$ content further increase to 4 vol%, as shown in Fig. 3g (area 1, 2, 3). This phenomenon is mainly caused by the high viscosity (> 1 Pa·s) of ceramic slurry, due to the addition of excessive fibers. Therefore, in order to guarantee that the tiny structures can be filled completely by the CaO-based ceramic slurry with a low viscosity, the $ZrO_{2\ (f)}$ content cannot exceed 3 vol% in the RIFT process to fabricate the ceramic mold with complex structures.

3.2 Microstructure and phase analysis

Figure 4a - Fig. 4d shows the fracture surface of the samples fabricated with different $ZrO_{2\,(f)}$ additions after sintered at 1400 ºC for 3 h. As shown in Fig. 4a-c, the $ZrO_{2\,(f)}$ are randomly arranged and homogeneously distributed in the CaO ceramic matrix when the content is not exceed 3 vol%; whereas, the $ZrO_{2\,(f)}$ are likely to distribute in fasciculate when the content is up to 4 vol%, as shown in Fig. 4d. The heterogeneous distribution of $ZrO_{2\,(f)}$ is caused by the insufficient dispersion of excess fiber in slurry. It can be noticed that the fibers length in the final composite are 60 ~ 70 μm on average, far shorter than the raw $ZrO_{2\,(f)}$, mainly caused by worn during the ball milling. In fact, in order to achieve better reinforcement, the damage to chopped fibers should be avoided. However, the ball milling, an effective and simple dispersion approach, is widely used for dispersion of high solid loading slurry with chopped fibers, which leads to the inevitable damage to chopped fibers. Therefore, it is very important to optimize the ball milling process, especially the duration of ball milling. In this study, the duration of ball milling is controlled in 40 min, to obtain a well-dispersed slurry without the severe damage of fibers.The primary toughening mechanism of the chopped fiber reinforced ceramic matrix composite is the fiber pulling-out, bridging and deboning. The fiber pulling-out and bridging can be obviously observed in Fig. 4a - d, and the deboning can be observed in Fig. 4e. The EDS was carried out to identify the composition on the interface of fiber and CaO matrix. According to the proportion of the elements distribution, as shown in Fig. 4f, it can be inferred that the main component of the interface on the fiber may be the calcium zirconate ($CaZrO_3$), formed by the reaction of CaO and ZrO_2 at elevated temperature, as shown in Eq. (2). It indicates that a strong interface is formed on the surface of fibers, which could transfer the load effectively and reinforce the mechanical properties. In addition, the layer of $CaZrO_3$ on the surface of $ZrO_{2\,(f)}$ fiber will also protect the internal $ZrO_{2\,(f)}$, preventing the further reaction of $ZrO_{2\,(f)}$ and the CaO matrix at an elevated temperature.

$$CaO + ZrO_2 \triangleq CaZrO_3 \qquad (2)$$

3.3 Mechanical properties and sintering shrinkage

Figure 6 shows the mechanical properties and sintering shrinkage of the samples fabricated with different $ZrO_{2\,(f)}$ content after sintered. As can be seen from Fig. 6a, both the room temperature (25 ºC) and elevated temperature(1200 ºC) bending strength increased with the $ZrO_{2\,(f)}$ content varying from 0 vol% to 3 vol% and peaked at 22.88 MPa and 15.74 MPa, respectively, when $ZrO_{2\,(f)}$ content is 3 vol%. Further increase the content of $ZrO_{2\,(f)}$ resulted in a slight decrease of bending strength due to the inhomogeneous microstructure of CaO-based ceramic sample caused by the heterogeneous distribution of excessive $ZrO_{2\,(f)}$. As can be seen from Fig. 6b, the elevated temperature (1200 ºC) deflection decreased as the $ZrO_{2\,(f)}$ content increased from 0 vol% to 3 vol% and the minimum deflection is 0.86 mm, when $ZrO_{2\,(f)}$ content is 3 vol%. A slight increase of deflection was exhibited with the further addition of the $ZrO_{2\,(f)}$ caused by the heterogeneous distribution of excessive $ZrO_{2\,(f)}$ as well. As can be seen from Fig. 6c-d, the apparent porosity increased from 29.46% to 31.42% and the sintering shrinkage decreased from 0.57% to 0.40% as the $ZrO_{2\,(f)}$ content increased from 1 vol% to 3 vol%. It indicates that

the chopped $ZrO_{2\ (f)}$ may well be formed in a bracket for the CaO ceramic matrix, and the CaO ceramic particles are fixed to retard the translocation of ceramic particles, so that the porosity of the ceramic mold increased and the sintering shrinkage decreased.

It showed that the mechanical properties and the sintering shrinkage could be significantly improved by the addition of $ZrO_{2\ (f)}$. The best comprehensive mechanical properties of elevated temperature (1200 ºC) bending strength of 15.74 MPa, elevated temperature (1200 ºC) deflection of 0.86 mm, sintering shrinkage of 0.40%, apparent porosity of 31.42%, which could excellently meet the requirements of investment casting, can be obtained when the addition of $ZrO_{2\ (f)}$ content is 3 vol%.

3.4 Case study

An CaO-based ceramic mold of impeller was fabricated by the RIFT with the $ZrO_{2\ (f)}$ content of 3 vol% according to the procedure described in Sect. 2, as shown in Fig. 7(a)-(d) and the internal structure of the mold was tested by industrial CT, as shown in Fig. 7(e)-(h). X-ray analysis reveals that the shape of the impeller was exactly duplicated and the internal structure of the impeller ceramic mold was well maintained, indicating that the CaO-based ceramic mold reinforced by chopped $ZrO_{2\ (f)}$ can meet the requirements of casting.

4. Conclusions

CaO-based integral ceramic mold with improved mechanical properties have been fabricated by SLA and TBA-based gel-casting with the chopped $ZrO_{2\ (f)}$ reinforced method. In order to obtain a sufficiently filled green body of CaO-based integral ceramic mold with tiny structure, the content of $ZrO_{2\ (f)}$ should not exceed 3 vol%. SEM and XRD analysis shows that the sample fabricated with the addition of $ZrO_{2\ (f)}$ content of 3 vol% has a microstructure with homogeneous distribution of $ZrO_{2\ (f)}$, which reinforce the CaO-based ceramic mold with fiber pulling-out, bridging and deboning. The room temperature (25 ºC) bending strength increased to 22.88 MPa, elevated temperature (1200 ºC) bending strength increased to 15.74 MPa, sintering shrinkage decreased to 0.40% and apparent porosity increased to 31.42% respectively. This CaO-based ceramic mold is an excellence candidate to be used in the investment casting for aerospace and engineering fields.

5. Declarations

Acknowledgements

The authors gratefully acknowledge the support of the Key Program of Equipment Pre-Research Foundation of China (Grant No. 61409230405). We thank Mr Zijun Ren at Instrument Analysis Center of Xi'an Jiaotong University for his assistance with SEM and EDS analysis.

6. References

[1] RICE R O Y W. CaO: I, Fabrication and Characterization. J Am Ceram Soc 1969, **52**: 420-427.

[2] Li Z, Zhang S, Lee W E. Improving the hydration resistance of lime-based refractory materials. Int Mater Rev 2008, **53**: 1-20.

[3] Ghosh A, Bhattacharya T K, Mukherjee B, et al. The effect of CuO addition on the sintering of lime. Ceram Int 2001, **27**: 201-204.

[4] Ghosh A, Bhattacharya T K, Maiti S, et al. Densification and properties of lime with V_2O_5 additions. Ceram Int 2004, **30**: 2117-2120.

[5] Ghasemi-Kahrizsangi S, Nemati A, Shahraki A, et al. Densification and properties of Fe_2O_3 nanoparticles added CaO refractories. Ceram Int 2016, **42**: 12270-12275.

[6] Hung C C, Lai P L, Tsai C C, et al. Pure titanium casting into titanium-modified calcia-based and magnesia-based investment molds. Mater Sci Eng A 2007, **454**: 178-182.

[7] Klotz U E, Heiss T. Evaluation of crucible and investment materials for lost wax investment casting of Ti and NiTi alloys. Int J Cast Metal Res 2014, **27**: 341-348.

[8] Fu B, Wang H, Zou C, et al. Interfacial reactions between Ti-1100 alloy and CaO crucible during casting process. T Nonferr Metal Soc 2014, **24**: 3118-3125.

[9] Liu F, Fan Z, Liu X, et al. Aqueous gel casting of water-soluble calcia-based ceramic core for investment casting using epoxy resin as a binder. Int J Adv Manuf Tech 2016, **86:** 1235-1242.

[10] Yang Q, Lu Z, Huang F, et al. The Preparation of Calcia-based Ceramic Slurry for Rapid Manufacturing Hollow Turbine Blade Based on Stereolithography. Proceedings of the 2nd International Conference on Progress in AM. Singapore: Research Publishing, 2016:158-163.

[11] Zhao H, Ye C, Fan Z, et al. 3D printing of CaO-based ceramic core using nanozirconia suspension as a binder. J Eur Ceram Soc 2017, **37**: 5119-5125.

[12] Hulse C O. Process of casting nickel base alloys using water-soluble calcia cores. U.S. Patent 3 643 728, Feb. 1972.

[13] Beruto D, Barco L, BELLERI G, et al. Vapor - Phase Hydration of Submicrometer CaO Particles. J Am Ceram Soc 1981, **64**: 74-80.

[14] Chen G, Li B, Zhang H, et al. On the modification of hydration resistance of CaO with ZrO_2 additive. Int J Appl Ceram Tec 2016, **13**: 1173-1181.

[15] Wu H, Li D, Guo N. Fabrication of integral ceramic mold for investment casting of hollow turbine blade based on stereolithography. Rapid Prototyping J 2009, **15**: 232-237.

[16] Wu H, Li D, Tang Y, et al. Rapid fabrication of alumina-based ceramic cores for gas turbine blades by stereolithography and gel-casting. J Mater Process Tech 2009, **209**: 5886-5891.

[17] Lu Z, Miao K, Zhu W, et al. Fractions design of irregular particles in suspensions for the fabrication of multiscale ceramic components by gel-casting. J Eur Ceram Soc 2018, **38**: 671-678.

[18] Yang Q, Zhu W, Lu Z, et al. Rapid Fabrication of High-Performance CaO-Based Integral Ceramic Mould by Stereolithography and Non-Aqueous Gel-casting. Materials 2019, **12**: 934.

[19] Hou Z, Du H, Liu J, et al. Fabrication and properties of mullite fiber matrix porous ceramics by a TBA-based gel-casting process. J Eur Ceram Soc 2013, **33**: 717-725.

[20] Hua Z, Yao G, Ma J, et al. Fabrication and mechanical properties of short ZrO_2 fibres reinforced $NiFe_2O4$ matrix composites. Ceram Int 2013, **39**: 3699-3708.

[21] Yang F, Zhang X, Han J, et al. Mechanical properties of short carbon fibres reinforced ZrB_2-SiC ceramic matrix composites [J]. Mater Lett 2008, **62**: 2925-2927.

[22] Zhang Y, Li S, Han J, et al. Fabrication and characterization of random chopped fibres reinforced reaction bonded silicon carbide composite[J]. Ceram Int 2012, **38**: 1261-1266.

[23] Tang S, Hu C. Design, preparation and properties of carbon fibres reinforced ultra-elevated temperature ceramic composites for aerospace applications: a review. J Mater Sci Technol 2017, **33**: 117-130.

[24] Liu H Y, Hou X Q, Wang X Q, et al. Fabrication of High-Strength Continuous Zirconia Fibers and Their Formation Mechanism Study. J Am Ceram Soc 2004, **87**: 2237-2241.

[25] Li L, Wang H, Su S. Porous Si_3N_4 ceramics prepared by TBA-based gel-casting. J Mater Sci Technol 2015, **31**: 295-299.

Figures

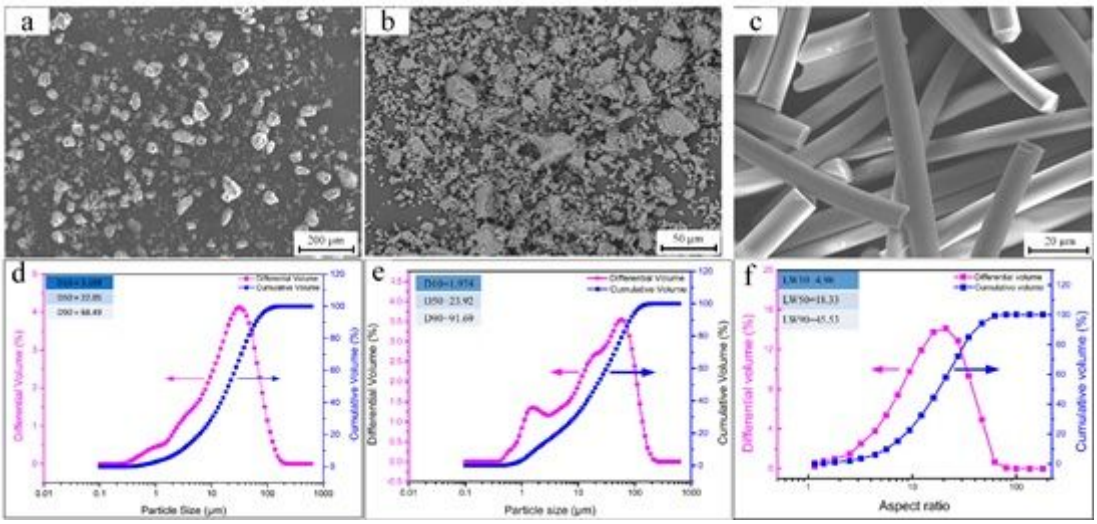

Figure 1

Characterizes of raw materials: (a) morphology of the CaO powders, (b) morphology of the MgO powders, (c) morphology of the ZrO2 (f), (d) particle size distribution of the CaO powders, (e) particle size distribution of the MgO powders, (f) aspect ratio of ZrO2 (f).

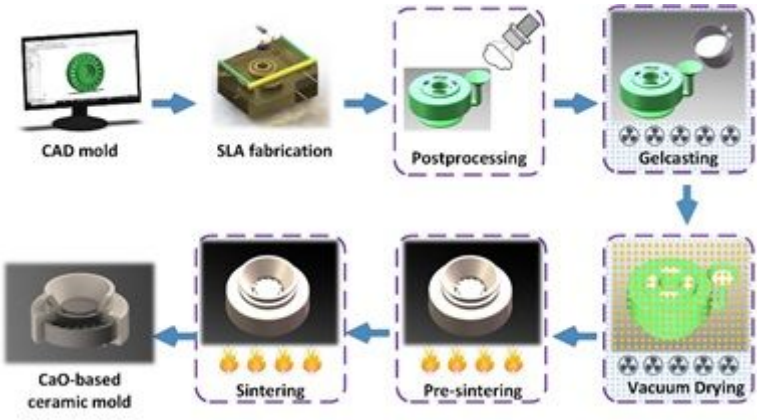

Figure 2

Fabrication flow chart of the CaO-based integral ceramic mold.

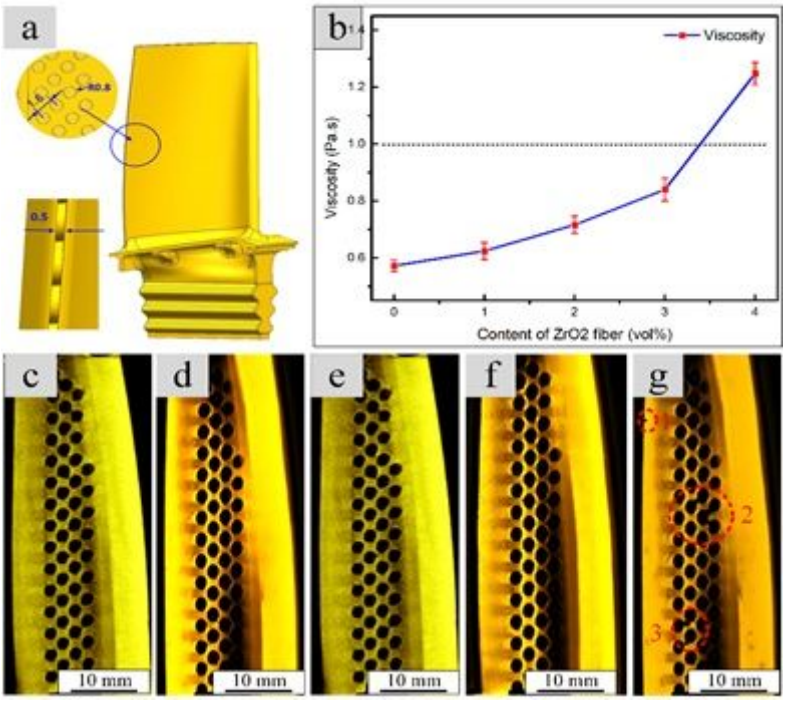

Figure 3

Effects of ZrO2 (f) content on viscosity and filling ability of the slurries: (a) viscosity of slurries with different ZrO2 (f) content, (b-f) CT images of different ZrO2(f) content: (b) 0 vol%, (c) 1vol%, (d) 2 vol%, (e) 3 vol%, (f) 4 vol%.

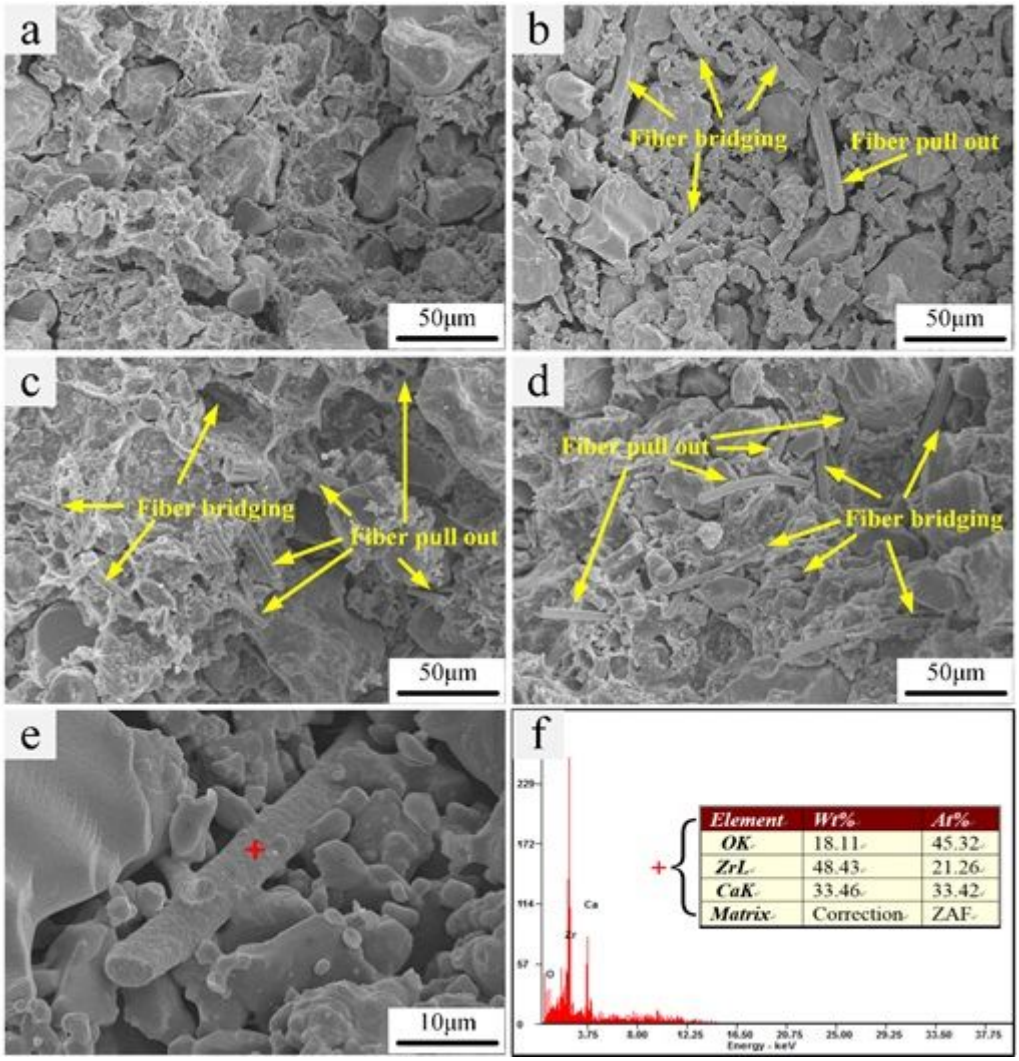

Figure 4

Microstructure of fracture surface with different ZrO2 (f) content: (a)1 vol%, (b)2 vol%, (c)3 vol%, (d)4 vol%,(e) (f) EDS of ZrO2 (f) interface.

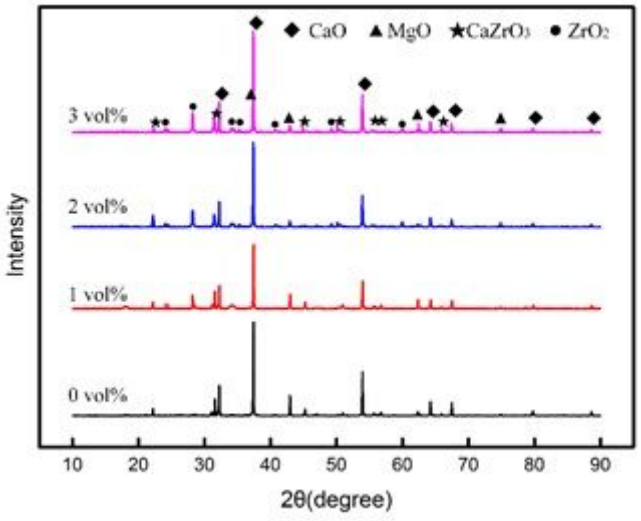

Figure 5

XRD Patterns of sintered ceramic mold with different ZrO2 (f) content.

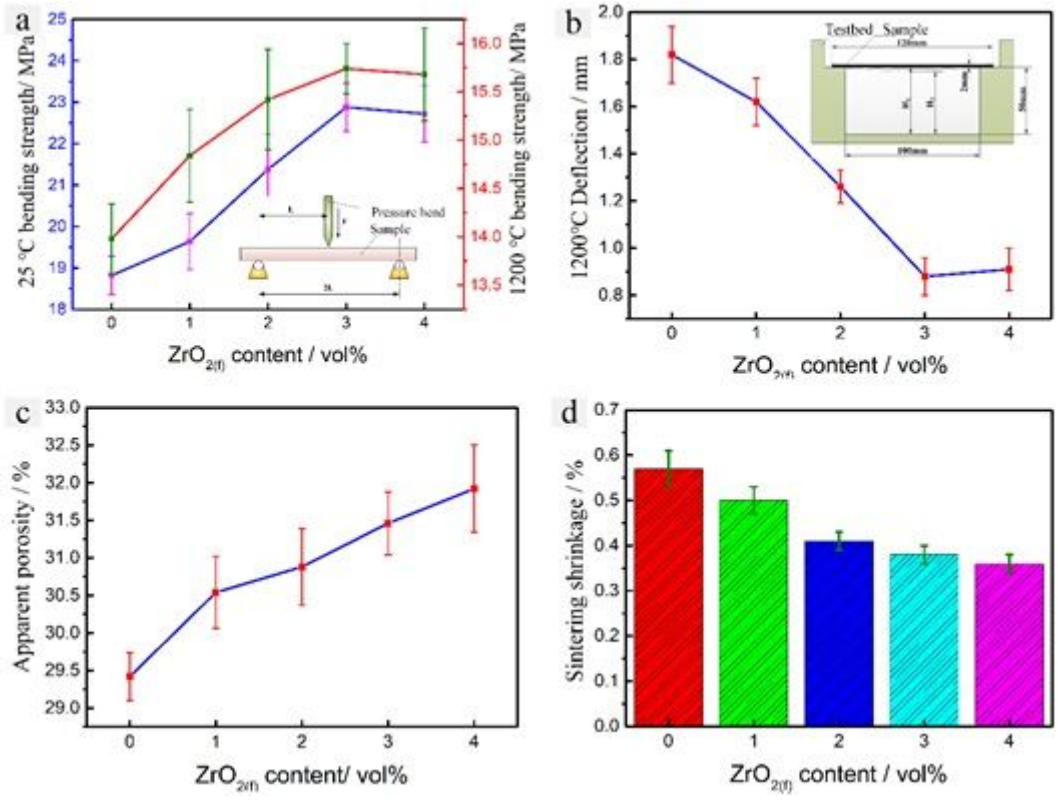

Figure 6

Effect of ZrO2 (f) content on properties of CaO-based ceramic mold: (a) room and elevated temperature bending strength, (b) elevated temperature deflection, (c) apparent porosity, (d) sintering shrinkage.

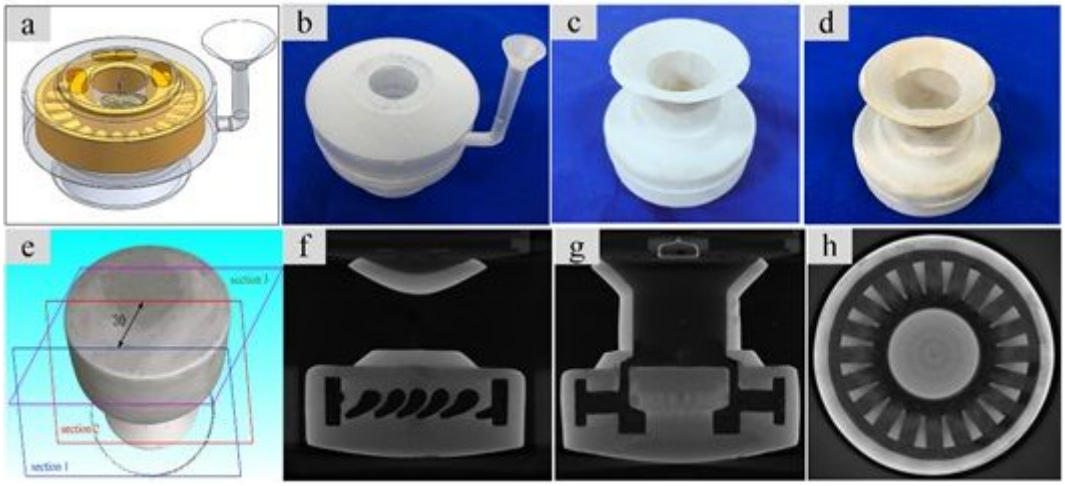

Figure 7

Fabrication of CaO-based ceramic mold of an impeller and the CT image of mold: (a) CAD mold, (b) resin mould, (c) dried green body, (d) sintered ceramic mold, (e) scan section of CT, (f) CT image of section 1, (g) CT image of section 2, (h) CT image of section 3.